Available online at www.sciencedirect.com

SciVerse ScienceDirect

Ceramics International 39 (2013) 3741–3745

CERAMICS INTERNATIONAL

www.elsevier.com/locate/ceramint

Facile synthesis and luminescent properties of $Y_2O_3:Eu^{3+}$ nanophosphors via thermal decomposition of cocrystallized yttrium europium propionates

Weifan Chen[a,*], Yuping Tong[b], Yue Liu[a], Ming Liu[a], Yucui Lin[a], Bin Gong[c], Zhishuang Cai[c], Xiaolin Zhong[c]

[a]School of Materials Science & Engineering, Nanchang University, Nanchang 330031, PR China
[b]School of Civil Engineering and Communication, North China University of Water Conservancy and Hydroelectric Power, Zhengzhou 450011, PR China
[c]Ganzhou Qiandong Rare Earth Group Co. Ltd., Ganzhou 341000, PR China

Received 10 September 2012; received in revised form 14 October 2012; accepted 15 October 2012
Available online 26 October 2012

Abstract

$Y_2O_3:Eu^{3+}$ nanophosphors were fabricated by direct thermal decomposition of monohydrate yttrium europium propionates, which can be facilely obtained via cocrystallization. The composition and structure of the cocrystallized product were confirmed by X-ray diffractionmetry (XRD), simultaneous differential scanning calorimetry (DSC) and thermogravimetric analysis (TGA) as well as inductively coupled plasma mass (ICP-MS) spectrometry. The effects of decomposition temperature on the resultant microstructures such as crystallinity, particle size and particle dispersibility were investigated by XRD and transmission electron microscopy (TEM). The dependence of their luminescent properties on decomposition temperature was also studied by fluorescence spectrophotometry. The results showed that the microstructures and luminescent intensities of $Y_2O_3:Eu^{3+}$ nanophosphors could be tuned by varying calcination temperatures of cocrystallized yttrium europium propionates from 600 to 1000 °C.

Keywords: Eu-dpoed yttria; Nanophosphors; Propionates; Thermal decomposition

1. Introduction

$Y_2O_3:Eu^{3+}$ is an efficient red-emission phosphor and has been widely used in fluorescent lamps (FL) and cathode ray tube (CRT) [1,2]. The studies during the last decade show that $Y_2O_3:Eu^{3+}$ nanophosphors has significant promise in field emission displays (FEDs) and plasma display panels (PDP) [3,4].

Many approaches have been developed for the fabrication of $Y_2O_3:Eu^{3+}$ nanostructures, such as precipitation [5–7], hydrothermal or solvothermal method [8,9], mechanochemical processing [10], spray pyrolysis [11], microemulsion [12], sol–gel [13] and combustion synthesis [14], etc. Among the various routes to the synthesis of $Y_2O_3:Eu^{3+}$ nanostructures based on thermal decomposition of precursors, two categories can be divided according to the precursor constitution, i.e. precipitates and gel. It is noticeable that the microstructures and physical properties of final products depend largely on the characteristics of the precursors obtained by controlled synthesis and the thermal decomposition conditions adopted. Therefore, choice and controlled synthesis of a suitable precursor is crucial to the fabrication of desired nanostructures with unique properties.

Numerous attempts have been made to synthesize $Y_2O_3:Eu^{3+}$ nanostructures via thermal decomposition of organometallic complex xerogel [13,15–17]. However, these efforts are limited to industrialized production due to complicated process, high cost and long synthetic duration. In our previous works, we have proposed a novel and simple method for the preparation of ultrafine and nanosized ceria particles via thermal decomposition, wherein

*Corresponding author. Tel.: +86 791 83969553; fax: +86 791 83969329.
E-mail address: weifan-chen@163.com (W. Chen).

0272-8842/$ - see front matter © 2012 Elsevier Ltd and Techna Group S.r.l. All rights reserved.
http://dx.doi.org/10.1016/j.ceramint.2012.10.210

the soluble crystalline hydrate cerium carboxylates were used as the precursors rather than the traditional precipitates and gel [18,19]. So far, to the best of our knowledge, there have been a few of reports about the thermal decomposition behavior of the rare earth propionates including Ce, La and Lu [19–21]. In this paper, we will put forward a novel and facile approach for the synthesis of Y_2O_3:Eu^{3+} nanophosphors via thermal decomposition of monohydrate yttrium europium propionates, which can be also easily obtained from cocrystallization. Their luminescent properties dependent on decomposition temperature have also been investigated. This method for synthesis of Y_2O_3:Eu^{3+} nanophosphors is based on thermal decomposition of soluble salt grains, which extends the scope of precursors besides precipitates and gel. Furthermore, due to many advantages such as easy operation, feasible cost and simple process, this new synthetic route to Y_2O_3:Eu^{3+} nanophosphors may find promising applications in the large scale production of Y_2O_3:Eu^{3+} nanophosphors.

2. Experimental procedures

2.1. Synthesis

Y_2O_3 (Purity: Y_2O_3/REO ≥ 99.999%) and Eu_2O_3 (Purity: Y_2O_3/REO ≥ 99.999%) were supplied by Ganzhou Qindong Rare Earths Group Co. Ltd. Propionic acid was of analytical grade and supplied by Sinopharm Chemical Reagent Co. Ltd. All the chemicals were used as received without further purification.

In a typical synthetic procedure, the mixture of Y_2O_3 and Eu_2O_3 with molar ratio of Y/Eu = 96.1/3.9 were completely dissolved in excess amount of propionic acid solution under continuous agitating and heating. Then, by repeating the processes of evaporating, cooling and filtering, all the large white crystals of yttrium europium propionates were crystallized out of the propionic acid solution. The final products were collected after the cocrystallized yttrium europium propionates were dried at 80 °C for 12 h and then calcined in a muffle furnace under air at the selected temperatures for 3 h.

2.2. Characterizations

Simultaneous DSC–TGA of the crystalline particles were conducted on a thermal analyzer (Model Q-600, TA Instruments) at a heating rate of 20 °C min^{-1} under static air from room temperature to 950 °C. The microstructures of the particles were observed via a transmission electron microscope (Model 200CX, JEOL Co.). Phase identification was performed on an X-ray diffractometer (Model D8 Advance, Bruker Co.) operating at 40 kV/50 mA using Cu-Kα radiation with a scanning speed of 0.15° 2θ per minute. Photoluminescence excitation (PLE) and photoluminescence (PL) properties of the samples were collected on a fluorescence spectrophotometer (Model F-4500, Hitachi Co.) at room temperature with a 300 W Xe-lamp as the light source. PMT voltage of the measurements was 400 V, the excitation and emission slits were set at 2.5 nm. The contents of Eu in the as-calcined samples were determined by ICP-MS spectrometer (Model ELAN DRC-e, Perkin Elmer, Inc.).

3. Results and discussion

In order to identify the phase of the grains crystallized from propionic acid solution of Y_2O_3 and Eu_2O_3, their XRD pattern was collected. As shown in the inset of Fig. 1, the characteristic peaks of the as-obtained grains are found to correspond well with those of monohydrate yttrium propionate (JCPDF 00-037-1559). Due to the small doping of Eu^{3+}, the characteristic peaks of monohydrate europium propionate were not observed. To further confirm the composition of the same sample, simultaneous DSC–TGA

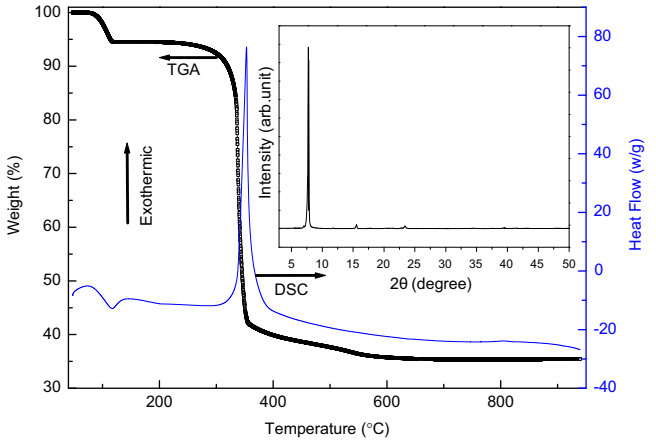

Fig. 1. DSC–TGA curves and XRD pattern (inset) of the crystalline particles obtained via dissolving mixture of yttria and europia (with molar ratio of Y/Eu = 96.1/3.9) with excess propionic acid and subsequent cocrystallization.

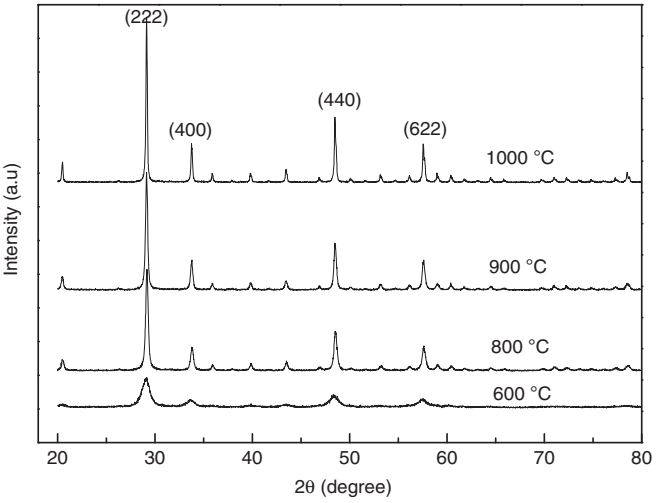

Fig. 2. XRD patterns of the samples obtained via decomposition of $Y_{0.961}Eu_{0.039}(C_2H_5COO)_3 \cdot H_2O$ at different temperatures for 3 h.

was conducted. As revealed in Fig. 1, the decomposition of hydrate crystalline salts on heating consists of three stages in weight loss. The first weight loss (5.48 wt%) before 120 °C results from the removal of one crystalline water, which is well consistent with the theoretical value of $Y_{0.961}Eu_{0.039}(C_2H_5COO)_3 \cdot H_2O$ (5.48 wt%). The second stage appears

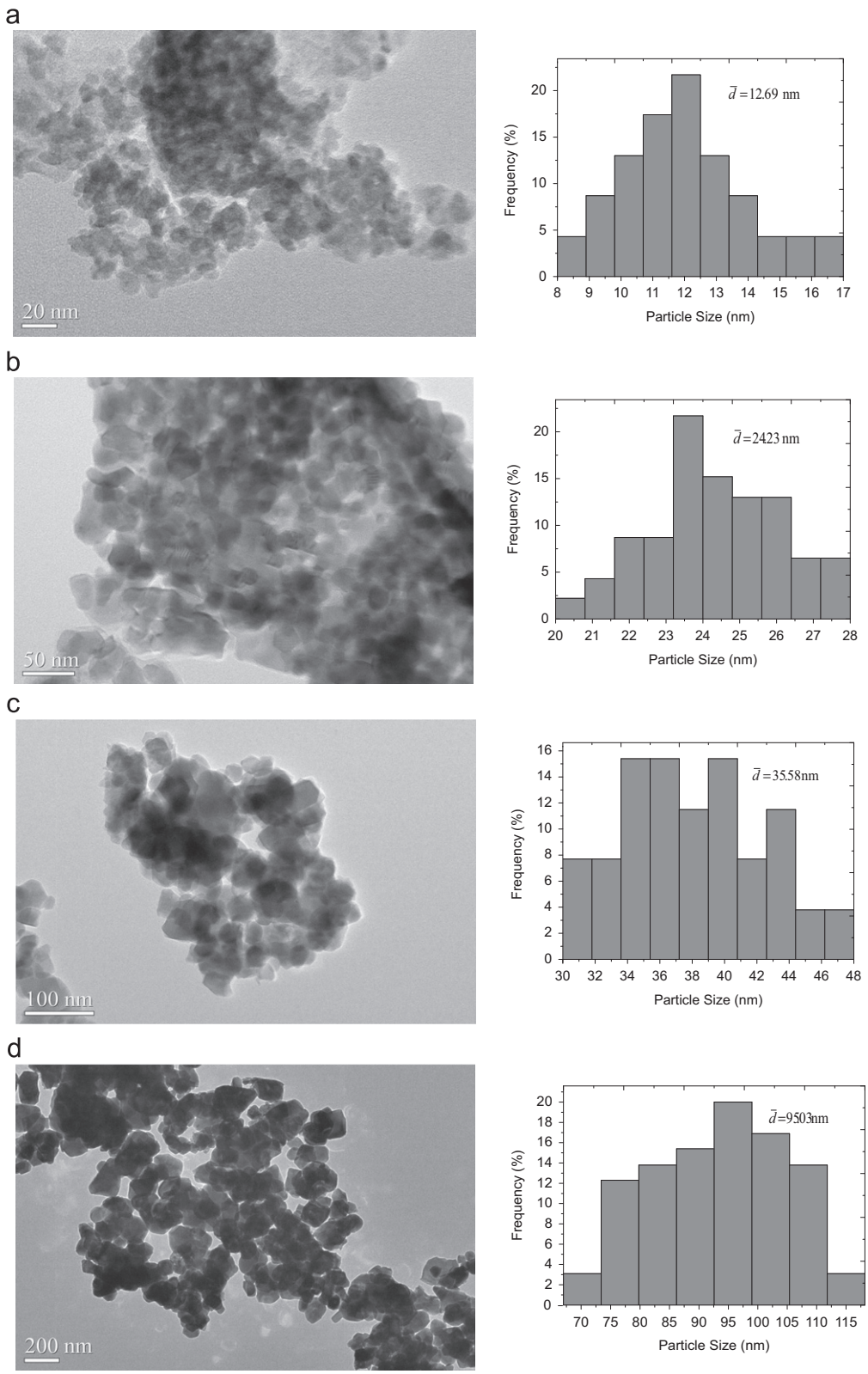

Fig. 3. TEM micrographs (left) and size distribution histograms (right) of the samples obtained via decomposition of $Y_{0.961}Eu_{0.039}(C_2H_5COO)_3 \cdot H_2O$ at different temperatures for 3 h: (a) 600 °C, (b) 800 °C, (c) 900 °C and (d) 1000 °C.

from 241.22 to 401.37 °C. A large weight loss in the TGA curve and a sharp strong exothermic peak at 353.01 °C in the DSC curve are observed simultaneously. This drastic exothermal process is ascribed to the decomposition of propionate group. Following this process is the third stage with gradual weight loss, which is possibly attributed to the further release of organic residues or carbon in the samples at higher temperature. The total weight loss is 64.64 wt%, which is in good agreement with theoretical value of 64.87 wt%. Moreover, the ICP-MS result confirms that the Eu content in the as-calcined sample agrees well with the designed Eu content. Based on the above data of XRD, DSC–TGA and ICP-MS, it can be concluded that the as-obtained crystalline grains are $Y_{0.961}Eu_{0.039}(C_2H_5COO)_3 \cdot H_2O$ and that the thermal decomposition processes of the yttrium europium propionates can be expressed as follows:

$$Y_{0.961}Eu_{0.039}(C_2H_5COO)_3 \cdot H_2O \rightarrow Y_{0.961}Eu_{0.039}(C_2H_5COO)_3 + H_2O\uparrow \quad (1)$$

$$Y_{0.961}Eu_{0.039}(C_2H_5COO)_3 + 21O_2\uparrow \rightarrow (Y_{0.961}Eu_{0.039})_2O_3 + 18CO_2\uparrow + 15H_2O\uparrow \quad (2)$$

Fig. 2 shows the XRD patterns of the samples obtained via calcination of $Y_{0.961}Eu_{0.039}(C_2H_5COO)_3 \cdot H_2O$ at different temperatures for 3 h respectively. All the characteristic diffraction peaks of the four samples are consistent with cubic Y_2O_3 (JCPDS card no. 25-1011). No additional phase was detected in the XRD patterns. As shown in Fig. 2, with variation of the sintering temperature from 600 to 1000 °C, the intensities of the characteristic diffraction peaks become stronger, indicating a higher crystallinity of Y_2O_3:Eu^{3+}.

To investigate the microstructure evolution of the as-calcined particles with sintering temperature, a transmission electron microscope was employed for observation. TEM micrographs of the samples obtained via calcination of $Y_{0.961}Eu_{0.039}(C_2H_5COO)_3 \cdot H_2O$ at different temperatures for 3 h are presented in Fig. 3. As can be seen, with the increase of calcination temperature, the primary spherical-shaped particles became larger and more dispersive, the average particle sizes of the samples from the correspondent particle size histograms grow from 12.69 nm at 600 °C, 24.23 nm at 800 °C, 35.58 nm at 900 °C to 95.03 nm at 1000 °C, which are approximately close to the average crystallite sizes calculated according to Scherrer's formula. Notably, it is at 1000 °C that the nanoparticle agglomeration improves remarkably although the particles become larger quickly. When the precursor was calcined above 1100 °C for 3 h, the resultant particles would grow to over 100 nm in size.

Photoluminescence excitation (PLE) and photoluminescence (PL) of $(Y_{0.961}Eu_{0.039})_2O_3$ calcined at different temperatures for 3 h are shown in Fig. 4(a). The broad yet strong band with a maximum at 254 nm observed from the PLE spectrum is attributed to the transition by charge transfer, that is, electronic transition from the 2p orbital of O^{2-} to the 4f orbital of Eu^{3+} activators [22]. Moreover, all

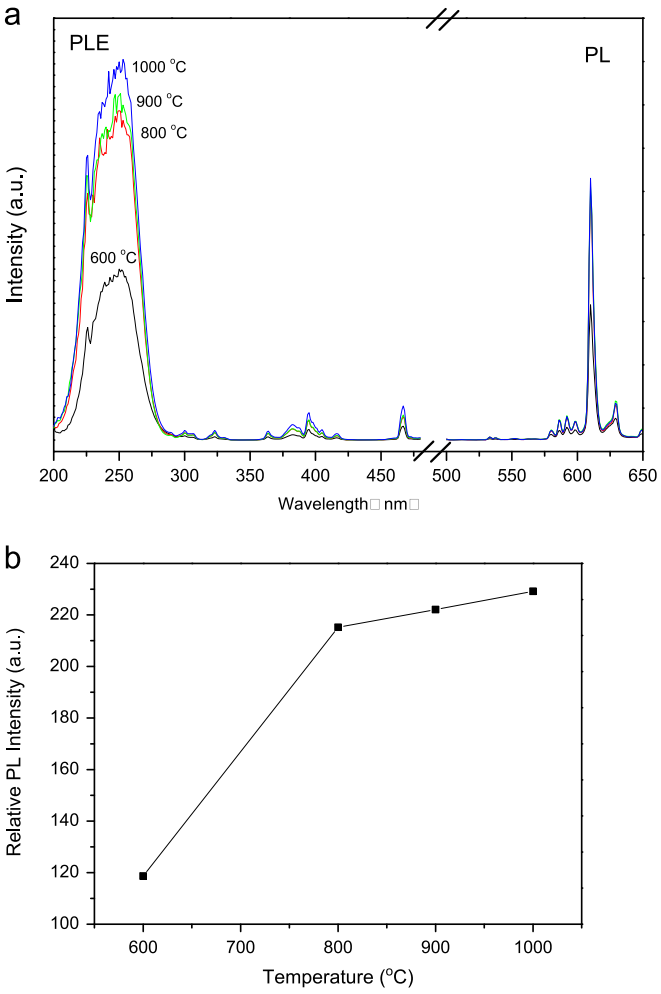

Fig. 4. (a) Room temperature PLE and PL spectra of the $(Y_{0.961}Eu_{0.039})_2O_3$ samples obtained via decomposition of $Y_{0.961}Eu_{0.039}(C_2H_5COO)_3 \cdot H_2O$ at different temperatures for 3 h; (b) The relative PL intensities of 610 nm emission as a function of calcination temperatures. The PLE spectra were obtained by monitoring the 610 nm emission while the PL spectra were obtained under UV excitation at 254 nm.

the samples exhibit emission at 610 nm corresponding to red emission due to $^5D_0 \rightarrow {}^7F_2$ transition under the excitation of 254 nm [12]. It can be seen from Fig. 4(b) that decomposition temperature of the precursor has significant affects on luminescence of the resultant particles, especially below 800 °C. A 200 °C increase in the temperature from 600 to 800 °C yields an 81% increase in the intensity of the 610 nm emission. This may be mainly due to a sharp increase of Y_2O_3:Eu^{3+} in crystallinity from 600 to 800 °C as can be seen in Fig. 2 [23].

4. Conclusions

We have developed a novel and simple route to Y_2O_3:Eu^{3+} nanophosphors via the thermal decomposition of soluble salt crystal grains, which can be easily obtained via dissolving the designated molar ration of yttria and europia with excess propionic acid and subsequent cocrystallization. DSC–TGA and XRD analysis confirm that the

as-obtained crystalline grains are Eu-doped monohydrate yttrium propionates. The results reveal that the calcination temperature has significant effects on size, agglomeration and luminescence of the resultant particles. It can be concluded that the luminescent intensities of Y_2O_3:Eu^{3+} nanophosphors may be adjusted by varying calcination temperature of cocrystallized yttrium europium propionates from 600 to 1000 °C. In prospect, this new synthetic route to Y_2O_3:Eu^{3+} nanophosphors may find promising applications in the large scale production of Y_2O_3:Eu^{3+} nanophosphors owing to such advantages as easy operation, feasible cost and simple process.

Acknowledgments

This work was financially supported by the National Natural Science Foundation of China (no. 21061011), the Scientific & Technological Research Project of Jiangxi Education Department (no. GJJ12034) and Ganzhou Qiandong Rare Earth Group Co. Ltd.

References

[1] M. Ilmer, G. Blasse, B.C. Grabmair, Luminescence of Bi^{3+} in gallate garnets, Chemistry of Materials 6 (1994) 204–206.
[2] C.R. Ronda, Phosphors for lamps and displays: an applicational view, Journal of Alloys and Compounds 225 (1995) 534–538.
[3] X. Jing, T. Ireland, C. Gibbons, D.J. Barber, J. Silver, A. Vecht, G. Fern, P. Trowga, D.C. Morton, Control of Y_2O_3: Eu Spherical particle phosphor size, assembly properties, and performance for FED and HDTV, Journal of the Electrochemical Society 146 (1999) 4654–4658.
[4] C.H. Kim, I.E. Kwon, C.H. Park, Y.J. Hwang, H.S. Bae, B.Y. Yu, C.H. Pyun, G.Y. Hong, Phosphors for plasma display panels, Journal of Alloys and Compounds 311 (2000) 33–39.
[5] J.G. Li, X.D. Li, X.D. Sun, T. Ishigaki, Monodispersed colloidal spheres for uniform Y_2O_3: Eu^{3+} red-phosphor particles and greatly enhanced luminescence by simultaneous Gd^{3+} doping, Journal Physics Materials Chemistry C 112 (2008) 11707–11716.
[6] X.R. Hou, S.M. Zhou, Y.K. Li, W.J. Li, Luminescent properties of nano-sized Y_2O_3:Eu fabricated by co-precipitation method, Journal of Alloys and Compounds 494 (2010) 382–385.
[7] R. Srinivasan, N.R. Yogamalar, J. Elanchezhiyan, R.J. Joseyphus, A.C. Bose, Structural and optical properties of europium doped yttrium oxide nanoparticles for phosphor applications, Journal of Alloys and Compounds 496 (2010) 472–477.
[8] S.L. Zhong, S.J. Wang, H.P. Xu, H.Q. Hou, Z.B. Wen, P. Li, S.P. Wang, R. Xu, Spindle like Y_2O_3:Eu^{3+} nanorod bundles: hydrothermal synthesis and photo- luminescence properties, Journal of Materials Science 44 (2009) 3687–3693.
[9] S. Yin, S. Akita, M. Shinozaki, R.X. Li, T. Sato, Synthesis and morphological control of rare earth oxide nanoparticles by solvothermal reaction, Journal of Materials Science 43 (2008) 2234–2239.
[10] D.M. Yang, D.C. Zhu., J. Zhuang, M.J. Tu, Synthesis and luminescent characteristic of Y_2O_3:Eu^{3+} nanocrystalline by mechanochemical process, Rare Metal Materials and Engineering 3 (2005) 1894–1896.
[11] Y.C. Kang, H.S. Roh, S.B. Park, H.D. Park, High luminescence Y_2O_3:Eu phosphor particles prepared by modified spray pyrolysis, Journal of Materials Science Letters 21 (2002) 1027–1029.
[12] M.H. Lee, S.G. Oh, S.C. Yi, D.D. Seo, J.P. Hong, C.O. Kim, Y.K. Yoo, J.S. Yoo, Characterization of Eu-doped Y_2O_3 nanoparticles prepared in nonionic reverse microemulsions in relation to their application for field emission display, Journal of the Electrochemical Society 147 (2000) 3139–3142.
[13] R.M. Krsmanović, Željka Antić, M.G. Nikolić, M. Mitrić, M.D. Dramićanin, Preparation of Y_2O_3: Eu^{3+} nanopowders via polymer complex solution method and luminescence properties of the sintered ceramics, Ceramics International 37 (2011) 525–531.
[14] Y.P. Fu, Preparation and characterization of Y_2O_3:Eu phosphors by combustion process, Journal of Materials Science 42 (2007) 5165–5169.
[15] M.I. Martinez-Rubio, T.G. Ireland, G.R. Fern, J. Silver, M.J. Snowden, A new application for microgels: novel method for the synthesis of spherical particles of the Y_2O_3:Eu phosphor using a copolymer microgel of NIPAM and acrylic acid, Langmuir 17 (2001) 7145–7149.
[16] L. Zhou, B. Yan, In situ synthesis and optical properties of strong red emitting nanomaterial: $Y_xGd_{2-x}O_3$: Eu^{3+} by composing different hybrid polymeric precursors, Ceramics International 32 (2006) 207–211.
[17] Y.Q. Zhai, Z.H. Yao, S.W. Ding, M.D. Qiu, J. Zhai, Synthesis and characterization of Y_2O_3:Eu nanopowder via EDTA complexing sol–gel process, Materials Letters 57 (2003) 2901–2906.
[18] Y.X. Li, C.M. Cheng, W.F. Chen, J.D. Hu, X.Z. Zhou, P.G. Hu, Preparation and polishing property of ultrafine ceria by calclning hydrate cerium acetate dlrectly, Chinese Journal of Inorganic Chemistry 22 (2006) 733–737.
[19] J.D. Hu, Y.X. Li, X.Z. Zhou, M.X. Cai, Preparation and characterization of ceria nanoparticles using crystalline hydrate cerium propionate as precursor, Materials Letters 61 (2007) 4989–4992.
[20] A. Kaddouri, C.J. Mazzocchia, Thermoanalytic study of some metal propionates synthesized by sol–gel route: a kinetic and thermodynamic study, Journal of Analytical and Applied Pyrolysis 65 (2002) 253–267.
[21] J.C. Grivel, Thermal decomposition of lutetium propionate, Journal of Analytical and Applied Pyrolysis 89 (2010) 250–254.
[22] M. Buijs, A. Meyerink, G. Blasse, Energy transfer between Eu^{3+} ions in a lattice with two different crystallographic sites: Y_2O_3:Eu^{3+}, Gd_2O_3:Eu^{3+} and Eu_2O_3, Journal of Luminescence 37 (1987) 9–20.
[23] C.H. Lee, K.Y. Jung, J.G. Choi, Y.C. Kang, Nano-sized Y_2O_3: Eu phosphor particles prepared by spray pyrolysis, Materials Science and Engineering: B 116 (2005) 59–63.